INSTITUTE OF PHYSICS PUBLISHING JOURNAL OF PHYSICS D: APPLIED PHYSICS

J. Phys. D: Appl. Phys. **36** (2003) 446–459 PII: S0022-3727(03)56429-4

Localized transitions in the thermoluminescence of LiF : Mg,Ti: potential for nanoscale dosimetry

Y S Horowitz[1,3], **L Oster**[2], **S Biderman**[1] **and Y Einav**[1]

[1] Physics Department, Ben Gurion University of the Negev, Beersheva 84105, Israel
[2] Negev Academic College of Engineering, Beersheva 84100, Israel

E-mail: yigal@bgumail.bgu.ac.il

Received 21 November 2002, in final form 10 January 2003
Published 14 February 2003
Online at stacks.iop.org/JPhysD/36/446

Abstract

We describe the effect of nanoscale spatially coupled trapping centre (TC)–luminescent centre (LC) pairs on the thermoluminescence (TL) properties of LiF : Mg,Ti. It is shown that glow peak 5a (a low-temperature satellite of the major glow peak 5) arises from localized electron–hole (e–h) recombination in a TC–LC pair believed to be based on Mg^{2+}–Li_{vac} trimers (the TCs) coupled to $Ti(OH)_n$ molecules (the LCs). Due to the localized nature of the e–h pair, two important properties are affected: (i) heavy charged particle (HCP) TL efficiency: the intensity of peak 5a relative to peak 5 following HCP high-ionization density irradiation is greater than that following low ionization density irradiation in a manner somewhat similar to the ionization density dependence of the yield of double-strand breaks (DSBs) induced in DNA. Our experimental measurements in a variety of HCP and fast neutron radiation fields have demonstrated that the ratio of glow peaks 5a/5 is nearly independent of particle species for the protons, deuterons and He ions investigated, is somewhat dependent on HCP energy, and is roughly 2–3 times greater than the peak 5a/5 ratio in low ionization density electron and photon fields. The intensity ratio of peak 5a/5 thus has the potential of estimating the ratio of dose deposited via high ionization density interactions compared to low ionization density interactions in a nanoscale volume without any prior knowledge of the characteristics of the radiation field, (ii) non-linear TL dose response: the relative lack of competitive processes in the localized recombination transitions leading to the TL of composite peak 5 versus the dose-dependent competitive processes in conduction band-mediated delocalized luminescence recombination leads to non-linear dose response (supralinearity) for composite peak 5 and a dependence of the supralinearity on ionization density. This behaviour is modelled in the framework of the unified interaction model (UNIM).

1. Introduction

Mixed-field radiation dosimetry involving heavy charged particle (HCP), fast neutron and gamma/electron radiation fields remains a highly intractable problem. Complex radiation fields of this nature are encountered in space, air-craft travel, nuclear reactors and, to a certain degree, in various types of radiobiological and medical applications. One dosimetric approach is to attempt to determine the particle type and energy spectrum of all the components of the radiation field and to correlate these with radiobiological end-points. But this seems a very difficult task [1, 2]. HCP and neutron fields are of enhanced radiobiological effectiveness (RBE) due to their high levels of ionization density resulting in increased

[3] Author to whom correspondence should be addressed.

radiation damage to biological systems. Radiation-sensitive targets in the human/mammalian cell are concentrated in the cellular nucleus and, in particular, the deleterious effects of ionizing radiation are known to arise from radiation damage to the DNA molecule either by direct ionization or indirectly via the action of hydroxyl radicals which are produced during water radiolysis [3]. HCPs and neutrons, are characterized as high linear energy transfer (LET) radiations, i.e. they produce an extremely dense lineal track of ionization and excitation events. Gamma rays and electrons, on the other hand, produce a more uniform distribution of ionization events and are considered to be low LET radiations. For example, the starting LET of a 5 MeV He ion in water is $\sim$95 keV micron^{-1} and the maximum LET at the end of the track is $\sim$230 keV micron^{-1}. These values are roughly an order of magnitude higher than the LET of commonly encountered gamma and electron radiation fields in the keV to MeV energy range. An LET of a few tens of keV micron^{-1} is commonly considered the approximate dividing line between low and high LET radiation. For example, Kampf [4] has studied the yield of SSBs and double-strand breaks (DSBs) induced in V79 as a function of LET (figure 1). The yield of DSBs reaches a maximum of $\sim 2 \times 10^{-11}$ breaks Gy^{-1} g^{-1} mol^{-1} at an LET of 100–200 keV micron^{-1} compared to $\sim 0.6 \times 10^{-11}$ breaks Gy^{-1} g^{-1} mol^{-1} at 10 keV micron^{-1}. Over the same range of LET, the yield of SSBs is approximately constant. A question of continuing interest is related to the different radiation action and damage of these two very different types of radiations in both biological and solid-state systems. Changes in the radiobiological response are expected when the local ionization density is increased to a level where multiple damage at the same site is likely to occur. For this reason much effort in the past has been invested in dosimetry aimed at the separation of mixed, complex, radiation fields into high LET and low LET components [5, 6]. This effort continues even though it is well known that LET cannot be correlated in a one-to-one correspondence with radiobiological effects because the ionization density does not depend in a unique manner on LET but rather on atomic number and LET. Apart from the lineal energy distribution, the radial dose distribution of HCPs also varies by many orders of magnitude in a few hundred angstroms, the radial dose distribution behaving approximately according to a r^{-2} law where r is the radial distance from the centre of the track. For example, the radial dose distribution of a 5 MeV He ion traversing LiF decreases from 1000 Gy (close to the track centre) to less than 10^{-2} Gy at a distance of approximately 500 Å from the track centre. In biological systems, chromosome breaks arise from DSBs of DNA which in turn are due to pairs of single-strand breaks (SSBs)—usually when these are produced in close proximity. Indeed the degree of irreversibility and/or the degree of function lethality may be correlated with the distance between the SSBs leading to the DSB. It is also believed that DSBs, as part of the so-called 'locally multiply damaged sites' (LMDs), contribute significantly to both the overall biological effects of 'low-LET' and 'high-LET radiation' and that they are responsible for most of the deleterious effects of 'high-LET' radiation. Clearly, however, a detailed understanding of the radiobiological end-points specific to these radiations is far from achieved [5, 6] and still represents an enormous challenge. It has been estimated that DSBs arise from SSBs in DNA whenever the SSBs are within approximately 10 base pairs (i.e. 3.4 nm) [6]. In general, a correlation has been found between DSBs and clusters of ionizations containing at least two to five ionizations in sites of diameters 1–4 nm [7]. It is, therefore, now generally accepted that energy concentrations and the microscopic spatial distribution of 'energy transfer points' in volumes of lineal dimensions of less than 10 nm are of critical significance in DNA damage. This, and the consequent inappropriateness of concepts based on 'track-averaged' quantities such as LET as a measure of DNA radiation damage, has led to an increasingly intensive search for a solid-state radiation device of nanometer dimensions [8] (the general shape of the DNA molecule being often approximated by a cylinder of approximately 2 nm diameter [9], as shown in figure 2.

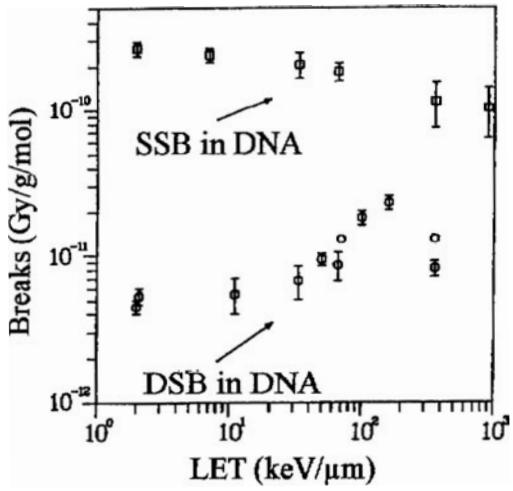

Figure 1. Yield of DSBs and SSBs induced in V79 cells as a function of LET (adapted from Kampf [4]).

The investigation of ionization density effects in the radiation effects/damage of thermoluminescence (TL) solid-state systems has been less intensive, however it is well known that here too, LET is not an entirely satisfactory parameter in the characterization of the HCP TL efficiency [10]. Figure 3 illustrates that the relative TL efficiency of composite peak 5 in LiF : Mg,Ti is dependent on the type of HCP, i.e. can vary by an order of magnitude at the same LET but for different particle species. In addition a saturation effect at high LET is observed very similar to the so-called 'Darmstadt hooks' in biological systems first observed in experiments in the Unilac Darmstadt and now confirmed for a large number of biological end-points [11]. In this paper we discuss a solid-state trapping centre/luminescent centre (TC/LC) molecular system in LiF : Mg,Ti of approximately nm dimensions [12] and similar in its behaviour, in some aspects, to the effects of ionization density in DNA. This similarity points to the potential of its use as a solid-state nanodosimeter in mixed radiation fields, even though it is likely that no single solid-state dosimeter will ever be able to simulate many of the extremely complicated SSB/DSB/LMD effects of radiation damage in DNA. In addition we describe the influence of localized transitions within this TC/LC system on the macroscopic dose response behaviour of the LiF : Mg,Ti system.

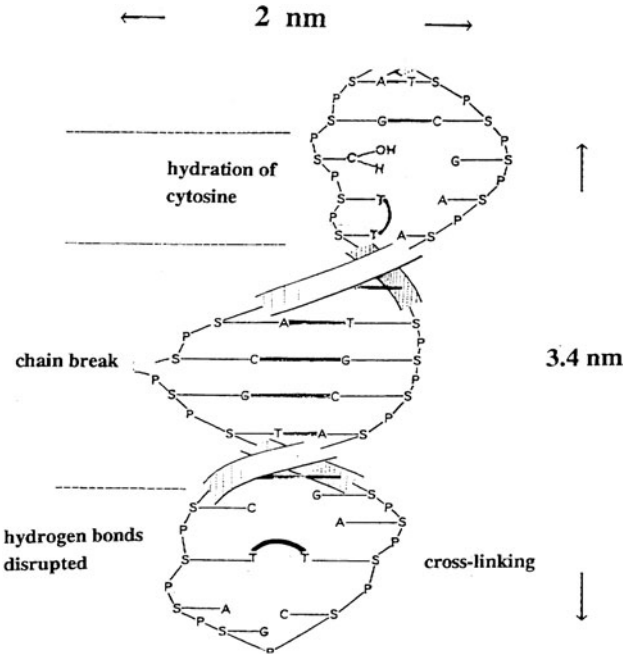

Figure 2. DNA molecule illustrating possible forms of radiation damage: chain breakage, base damage and cross-linkage (adapted from Deering R A 1962 *Sci. Am.* **207** 144).

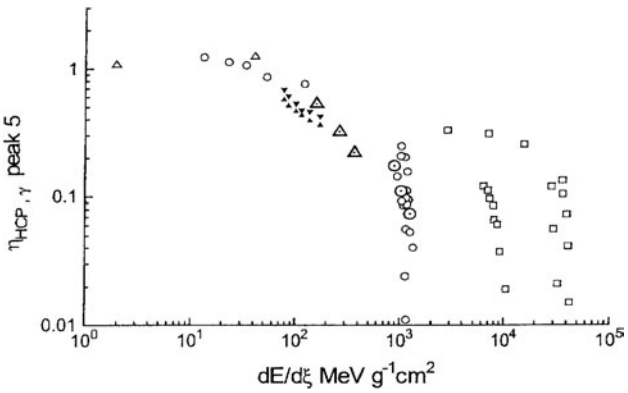

Figure 3. Relative TL efficiency with respect to ^{60}Co for the composite peak 5 signal for several types of HCPs (protons (△), He (○), heavier ions (□) (from Horowitz *et al* [10]).

2. Defect structures in LiF : Mg,Ti

As is well known, the dosimetric properties of TL materials are intimately related to their defect structure. Prior to the description of defect creation mechanisms by irradiation it is useful to describe, albeit in great brevity, the defect structure of the material in thermodynamic equilibrium. An important example, is LiF : Mg,Ti, which due to its dosimetric prominence, has been the most intensively investigated of all the TL materials.

LiF consists of two interpenetrating fcc lattices, one for Li^+ and one for F^- ions (figure 4). Each Li^+ ion located in the centre of a cube is surrounded by six nearest F^- ions and each F^- ion is similarly surrounded by Li^+ ions. The ions are closely packed with a lattice constant of 0.4 nm. Thermodynamic defects consist of Schottky defects (pairs of

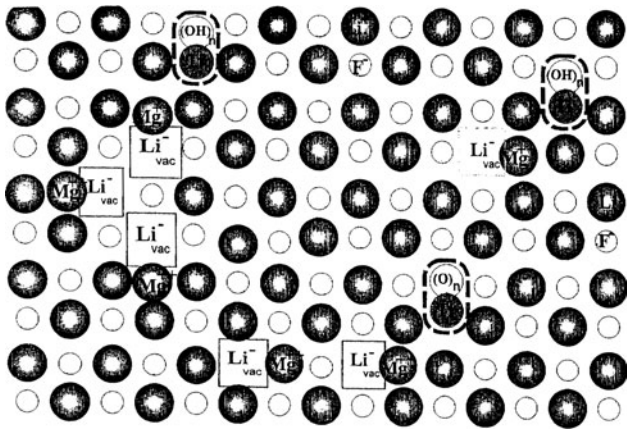

Figure 4. Crystal structure of LiF : Mg,Ti illustrating the molecular structure of the spatially correlated TC/LC structure responsible for composite peak 5. The inter-atomic distance between neighbouring Li^+ and F^- ions is 0.2 nm. The structure responsible for composite peak 5 is composed of three Mg^{2+}–Li_{vac} dipoles (forming a trimer—the TC) coupled to $Ti(OH)_n$ (the LC). The size of the TC/LC cluster has been estimated at approximately ten inter-atomic distances, i.e. 2 nm.

Li^+ and F^- vacancies) and Frenkel defects (Li^+ or F^- vacancy-interstitial pairs) with the latter becoming important only at high temperatures. Mg^{2+} substitutes Li^+ with charge neutrality being preserved by the presence of excess Li^+ vacancies. This results in impurity vacancy pairs (Mg–Li_{vac}) or dipoles which in turn form clusters to minimize the crystal's free energy. The most important clusters are trimers which consist of three dipoles. High temperature annealing and usually applied cooling rates following heating of the material results in most of the Mg in the form of trimers or in Mg precipitates. The solid-state reactions can be summarized as:

$$\text{Free } Mg^{2+} + Li^-_{vac} \Leftrightarrow \text{dipoles} \Leftrightarrow \text{trimers} \Leftrightarrow \text{precipitates}$$

Titanium enters the LiF substitutionally for Li^+ as Ti^{3+} or Ti^{4+} . Charge compensation takes place by several methods, among them formation of $Ti^{4+}(O^{2-})_3$ and $Ti(OH)_n$ complexes and formations of OH^- ions which cluster with Mg to form $Mg(OH)_m$ complexes. Such complexes reduce the TL emission from this material probably by the formation of centres which compete with TL related centres. Thus $(OH)^-$ plays a conflicting role, producing complexes for luminescence ($Ti(OH)_n$) and competing complexes ($Mg(OH)_m$) [13].

The primary products of ionizing radiation are the electrons, holes and excitons. It is necessary for defects to be created in order that the energy possessed by the pairing of an electron and a hole or by an exciton is dissipated locally. Products are neutral Frenkel pairs, charged Frenkel pairs and Schottky pairs. Mechanisms of formation include double ionization and single ionization. Irradiation of LiF : Mg,Ti induces several radiation-induced centres, most of them associated with the ones mentioned above present in thermodynamic equilibrium. Their precise identity is still a question of considerable debate, however, the main dosimetric peak 5 has been identified as a Mg–Li_{vac} trimer [14]. For a detailed discussion of the roles of defects in the TL of LiF : Mg,Ti, the reader is referred to Stoebe and Morgan [15].

3. Spatially correlated TCs and LCs in LiF : Mg,Ti (TLD-100)

The electron TCs and the hole trapping recombination LCs responsible for the major dosimetric glow peaks in LiF : Mg,Ti are spatially correlated, i.e. loosely coupled together by a long-range interaction into a TC/LC molecular complex. The existence of this complex was first pointed out following measurements of the emission spectra of LiF during TL [16] which demonstrated that Ti complexes responsible for the luminescence are modified by the aggregation state of the Mg in Mg-doped crystals. Thus unperturbed Ti centres give rise to emission near 410–420 nm which is the main emission band observed. Ti(OH) centres near Mg dipoles, however, emit near 460 nm while those near Mg trimers emit near 420 nm. Townsend *et al* based these conclusions on the observation that TL peaks [2, 3, 5, 6] (believed to arise from different configurations of Mg–Li_{vac} dipoles, dimers and trimers) do not emit at the same wavelength, in fact there was a general shift in wavelength to lower values as the peak temperature increased. Recent high sensitivity and resolution studies [17] together with computerized deconvolution indicate that the common set of the emission bands for the different TL peaks does not change, but that the relative intensities of the different emission bands are changed as a function of sample temperature, thus leading to what had previously appeared to be [16] a shift in emission wavelength. The underlying mechanism to explain the emission spectral variations, however, remains the same and is most likely due to varying degrees of TC/LC coupling/perturbation. These emission spectrum studies were followed by detailed mixed order kinetic studies of the shape of the glow peaks which show that the thermal activation energy of the TC responsible for peak 5 in LiF : Mg,Ti single crystals is a function of Ti concentration [18]. This behaviour would not occur if the TCs (based on Mg defects) and the LCs (based on Ti defects) were independent entities.

4. The spatially correlated TC/LC model for composite peak 5

It has been recently demonstrated by T_m–T_{stop} studies following He ion irradiation that glow peak 5 is actually a composite structure composed of three overlapping glow peaks, labelled 5a, 5 and 5b as shown in figure 5 [19]. For glow curve heating rates of approximately 1.5°C s^{-1}, the temperatures at maximum intensity, (T_m) of peaks 5a, 5 and 5b are 193°C, 210°C and 224°C, respectively. In similar analyses using gamma rays it proved very difficult to observe the presence of peak 5a due to its low intensity relative to peak 5 in the glow curve (figure 6). T_m–T_{stop} analysis is a method of peak resolution often used as a first and critical step in the deconvolution of complex glow curves. The sample following irradiation is heated to a sufficiently high temperature (T_{stop}) in order to readout almost the entire glow curve. The residual, belonging only to the highest temperature glow peak, is obtained by a second readout and analysed. The entire procedure is repeated at a slightly lower temperature. As T_{stop} is decreased more glow peaks are required to analyse the residual obtained by second readout. The deconvolution procedure of the residual glow curve yields the maximum

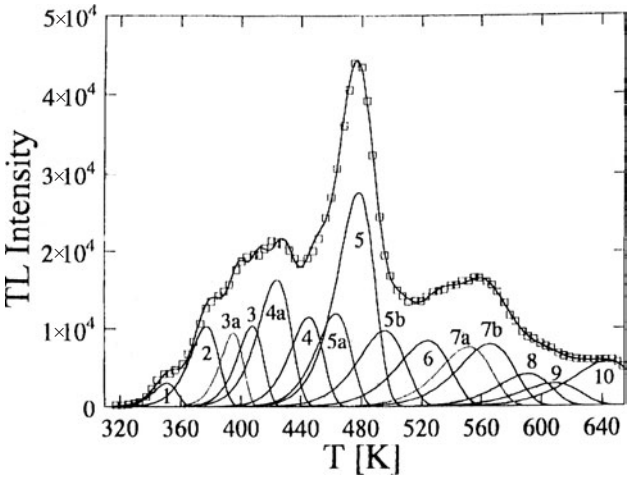

Figure 5. Deconvoluted glow curve of LiF : Mg,Ti following irradiation by 6.8 MeV He ions. The glow curve is considerably more complex than that following low ionization density photon/electron irradiation (previously published as figure 1 in Horowitz Y S *et al* 2002 *Radiat. Prot. Dosim.* **100** 95–8).

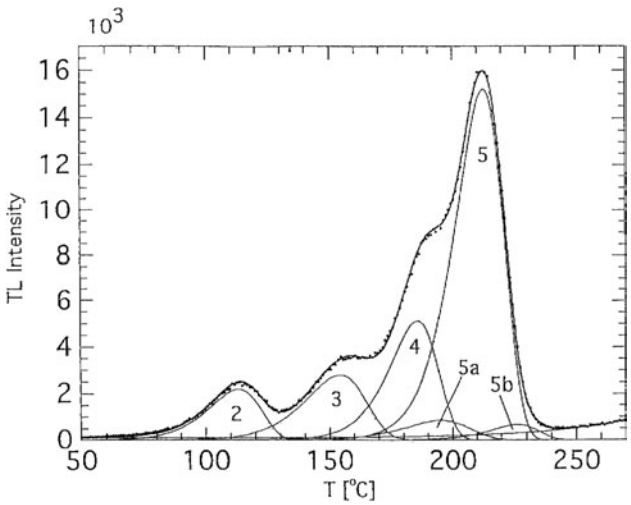

Figure 6. A typical deconvoluted glow curve of LiF : Mg,Ti (TLD-100) following low dose (low ionization density) gamma rays. The maximum intensity of peak 5a occurs at a temperature, T_m, 17 ± 1°C lower than the major dosimetric peak and its intensity is approximately 10% that of peak 5.

temperature of the glow peaks as well as the activation energy associated with each glow peak. A plot of T_m against T_{stop} reveals a 'staircase' shaped pattern where each region corresponds to the presence of an individual peak. The results of this procedure following He ion irradiation are shown in figure 7 [19] and constituted the first convincing evidence for the composite nature of peak 5. As previously mentioned, peak 5a is not readily observed following gamma irradiation but computerized glow curve deconvolution employing strictly controlled analysis protocols and using ancilliary thermal and optical bleaching techniques to characterize and simplify the glow curve and its components has allowed the determination of the relative intensity following gamma ray irradiation at 0.08 ± 0.008 (1 SD) [20]. Computerized glow curve analysis indicates that the relative intensity of peak 5a to peak 5 following 1 MeV amu^{-1} He ion irradiation is 0.34 ± 0.04

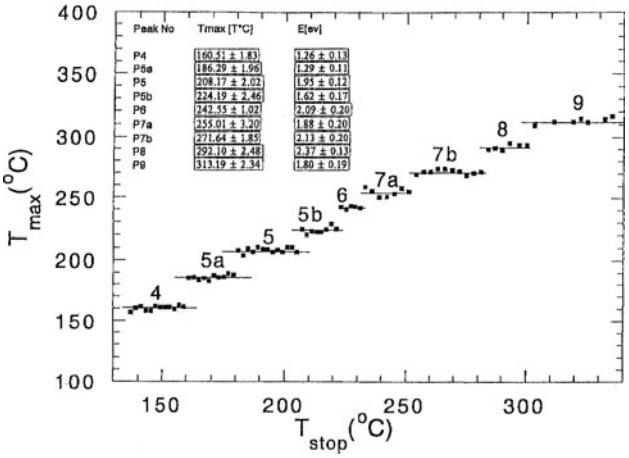

Figure 7. The results of T_m–T_{stop} measurements following irradiation by He ions. Note the staircase-shaped pattern and the strong presence of peak 5a (previously published as figure 2 in Horowitz Y S *et al* 2002 *Radiat. Prot. Dosim.* **100** 95–8).

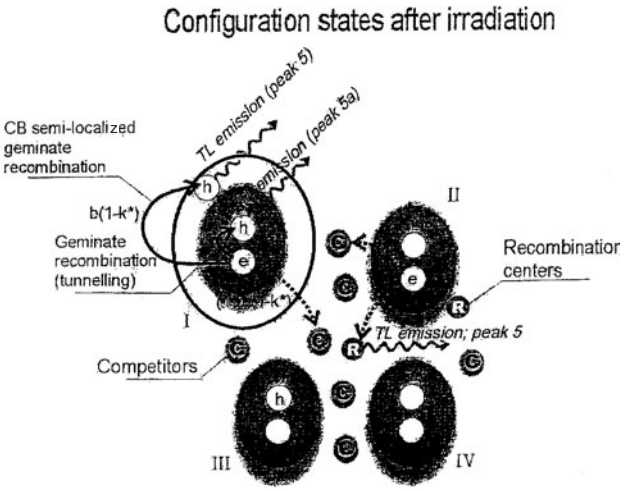

Figure 8. Schematic representation of the TC/LC spatially correlated model involving both geminate (localized) recombination and recombination via CB mechanisms. Each large oval represents a spatially correlated TC/LC complex. Following irradiation, the complex can be populated in the four different configurations as shown: I—captured electron and hole, II—electron-only, III—hole-only, IV—empty configuration. R represents recombination centres and C represents CCs. The relation $k = k^* + b(1 - k^*)$ is demonstrated, where k^* is the fraction of processes leading to geminate recombination between a locally trapped e–h without involvement of the CB. The fraction $1 - k^*$ of the trapped electrons in configuration I escape to the CB upon heating and $b(1 - k^*)$ recombine locally and are not subject to competitive processes. The fraction $(1 - k^*)(1 - b)$ are subject to competitive processes and may in fact be indistinguishable from electrons released from configuration II. Two routes for recombination are also shown: (i) the electron recombines with the hole within the complex (⟶) giving rise to peak 5a, (ii) recombination of electron from either electron occupied configuration with an external LC, with possibility of competition due to CB transport (- - ->) giving rise to peak 5. At low dose levels (in the linear part of the dose response region), the processes represented by k^*, and $(1 - k^*)b$ are postulated to give rise to peak 5a and 5, respectively.

(1 SD) [20]. Other evidence has also accumulated indicating the presence of peak 5a. For example, Delgado and Gomez-Ros [21], on the basis of experimental measurements of the isothermal decay of peak 5 at 165°C, maintained that there must exist another low intensity peak sandwiched between peaks 4 and 5. It has been previously suggested [22] that peak 5a arises from geminate recombination between a locally trapped electron–hole (e–h) in the TC/LC pair and peak 5 arises from the capture of an electron only. Peak 5b may be generated by a TC which has captured an electron and which is at the other end of the distribution of coupling strengths, i.e. it is very weakly or not coupled to an LC at all. Peak 4, ($T_m = 184$°C) on the other hand, is considered to arise from the same basic TC/LC configuration which has captured a hole only. Thus composite peak 5 as well as peak 4 arises from the spatially correlated/coupled TC/LC structure where the strength of the coupling/distance between the TC/LC pair varies from the extreme of strong coupling (highly localized TC/LC) to very weak or no coupling (independent TCs and LCs). This proposal is in-line with renewed emphasis on extended defect models of TL [23] in which it has been shown that long range coupling between TC/LC pairs can exist over some 50 neighbouring ion shells and influence over a thousand neighbouring ions. Thus, a probability distribution function exists for the likelihood of finding the trapped electron and hole at various distances of separation. When the distances are very large (say, greater than some several nms) the complex acts essentially as two independent centres and e–h recombination occurs via charge carrier migration in the conduction band (CB). It can be estimated to a first approximation that the average distance between Mg based complexes in LiF : Mg,Ti (∼150 ppm Mg-wt.%) is ∼6 nm [24] so that this distance must be a measure of the upper limit on the physical size of the TC/LC complex. When the TC/LC separation is above a certain threshold, the trapped electron following thermal excitation is elevated to the CB, migrates in the crystal, and may reach LCs or be annihilated by competitive processes leading to non-luminescent recombination. The electron in the CB is thought of as an almost completely delocalized entity and has no recollection of the specific site from which it was thermally liberated. This delocalized process is believed to be the major mechanism giving rise to the main dosimetric glow peak 5 in LiF : Mg,Ti (TLD-100) as shown in figure 8. Due to the delocalized nature of the CB recombination mechanism, there can be no defined site-size appropriate to the entire TL mechanism giving rise to glow peak 5. On the other hand, as the distance between the trapped electron in the TC and trapped hole in the LC decreases, a different, localized, recombination mechanism, termed 'geminate recombination', comes into play. This type of luminescent recombination occurs directly via a quantum-mechanical tunnelling process or via short-range, quasi-localized, migration in the CB between nearest-neighbour TCs and LCs. It is interesting to note that the emission spectra (consisting of five emission bands at 2.49, 2.64, 2.84, 3.1 and 3.59 eV) of composite peak 5 does not change significantly over the temperature range of composite peak 5 TL [17]. This indicates that the same LC(s) are active in the luminescence mechanism of peaks 5a, 5 and 5b. One could have expected that the strong TC/LC coupling appropriate to peak 5a would result in a perturbation of the emission spectrum in the vicinity of peak 5a TL—however, the weak relative intensity of peak 5a and the

strongly overlapping emission bands renders this difference (if it exists) impossible to detect. Finally, one should note that the tunnelling mechanism is not unknown in TL processes and has recently been reviewed by Visocekas [25]. The tunnelling recombination probability, predicted by the degree of overlap of the two wavefunctions of the pair, is strongly dependent on the thickness of the potential barrier which indicates relatively small distances between the coupled TC and LC, certainly no greater than the order of tens of angstroms. This process, we believe, gives rise to the new glow peak, labelled peak 5a, which is the solid-state conceptual equivalent of the DNA DSB, since it arises from two localized energy transfer events leading to the simultaneous capture of the electron and hole. As in DSB damage in DNA, the threshold distance defining the appearance of geminate recombination leading to peak 5a is estimated to be approximately 2–3 nm; as in DNA, the geminate recombination occurs over a well-defined, nm-sized-volume encompassing the first-nearest-neighbour TC/LC spatially correlated molecule.

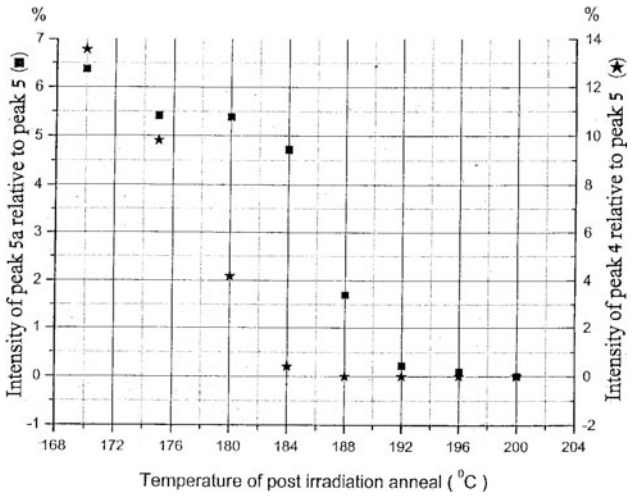

Figure 9. Relative intensities of peak 5a and peak 4 to peak 5 as a function of the temperature of post-irradiation annealing (previously published as figure 1 in Horowitz Y S *et al* [27]).

5. Experimental evidence for the e–h nature of peak 5a

The experimental evidence supporting the premise that peak 5a arises from simultaneous e–h capture in a spatially correlated TC/LC pair is described in the following.

5.1. Conversion efficiency studies

The conversion efficiency (CE) of any of the low-temperature glow peaks to peak 4 following optical excitation, is given by

$$\mathrm{CE} = \frac{I_4(t) - I_4(t=0)}{I_i(t=0) - I_i(t)}, \tag{1}$$

where $I_4(t)$, $I_i(t)$ are the integrals of glow peaks 4 and $i = 2$, 3, 5a, 5 after a bleach of duration t and $I_4(t=0)$, $I_i(t=0)$ are the glow peak intensities before the bleach. We have experimentally measured a very high CE ($\mathrm{CE}_{5a\to4} = 3 \pm 0.5$) of peak 5a to peak 4 deduced from detailed optical bleaching studies at 310 nm (4 eV) as a function of the temperature of post-irradiation annealing, compared to the much lower CE of peak 5, ($\mathrm{CE}_{5\to4} = 0.0026 \pm 0.012$) [26, 27].

5.1.1. Experimental procedures. Illumination of LiF : Mg,Ti with 310 nm (4 eV) light causes composite peak 5 to decrease due to the ionization of electrons, and it is also observed that peak 4 simultaneously increases. The choice of 310 nm light is dictated by the observation that gamma irradiation of LiF TLD-100 produces two strong optical absorption bands at 380 nm (5 eV) and 310 nm (4 eV) which are absent in undoped LiF. There is considerable evidence to associate the 4 eV band with composite glow peak 5 [28, 29] and the 5 eV band with the F centre. Dosimetry grade LiF (TLD-100) chips ($3 \times 3 \times 0.38\ \mathrm{mm}^3$) originating from Harshaw/Bicron were used for all the experiments. The light source employed was a 300 W xenon lamp attached to an Oriel $\frac{1}{8}$ m monochromator with 1200 lines mm^{-1} grating and 0.76 mm entrance and exit slits. The output intensity at 310 nm was 0.3 mW cm^{-2}. Irradiations were carried out with a $^{90}\mathrm{Sr}/^{90}\mathrm{Y}$ beta source (9 Gy h^{-1} in LiF) to dose levels of 10 and 100 Gy. In order to study the CE of the various glow peaks, post-irradiation annealing of 6 s duration was carried out in a N_2 atmosphere from 170°C to 200°C in intervals of 4–5°C. The effect of the post-irradiation anneals on the glow peak intensities is shown in figure 9. At a PIA of 184°C, peak 4 ($T_\mathrm{m} = 184$°C) has been almost completely erased but peak 5a maintains an intensity of 5% relative to peak 5. At 192°C and above, peak 5a ($T_\mathrm{m} = 193$°C) is also reduced to negligible intensities and only peaks 5 and 5b remain in the glow curve.

Effects of illumination: Examples of the effect of illumination by 310 nm light for 12 h on the glow curves at three different (PIA) temperatures are shown in figure 10. At a PIA of 170°C, both peaks 4 and 5a are present in the glow curve. Following the bleach, peak 4 has grown substantially, and is now by far the dominant glow peak; peak 5a has been totally erased and peak 5 has been reduced to 15% of its original intensity. At a PIA of 184°C, peak 4 is not present in the glow curve before the bleach; following the bleach it is again the dominant glow peak; peak 5a has been totally erased and again peak 5 has been reduced to 15% of its original intensity. The growth of peak 4 however does not occur following a bleach at 200°C. Before the bleach, only peak 5 appears in the glow curve. The 12 h bleach again reduces peak 5 to 15% of its pre-bleached intensity, but peak 4 is only very slightly regrown by the bleach. These results unequivocally establish that the peak 5a traps are those which are efficiently converting to peak 4 traps by optical excitation. The strong regrowth of peak 4 is observed only over the temperature region where peak 5a exists in the pre-bleached glow curve. Following computerized glow curve deconvolution of the pre-bleached and post-bleached glow curves; the CE of peak 5a is measured to be 3 ± 0.5 and is *three orders of magnitude greater* than the CE of peak 5 to peak 4.

The extremely high CE of peak 5a to peak 4 following 4 eV optical excitation is strong evidence for the e–h trapping nature of the peak 5a TC/LC configuration. The decrease of the CE with post-irradiation annealing temperature, illustrated in figure 11, demonstrates that composite glow peak 5

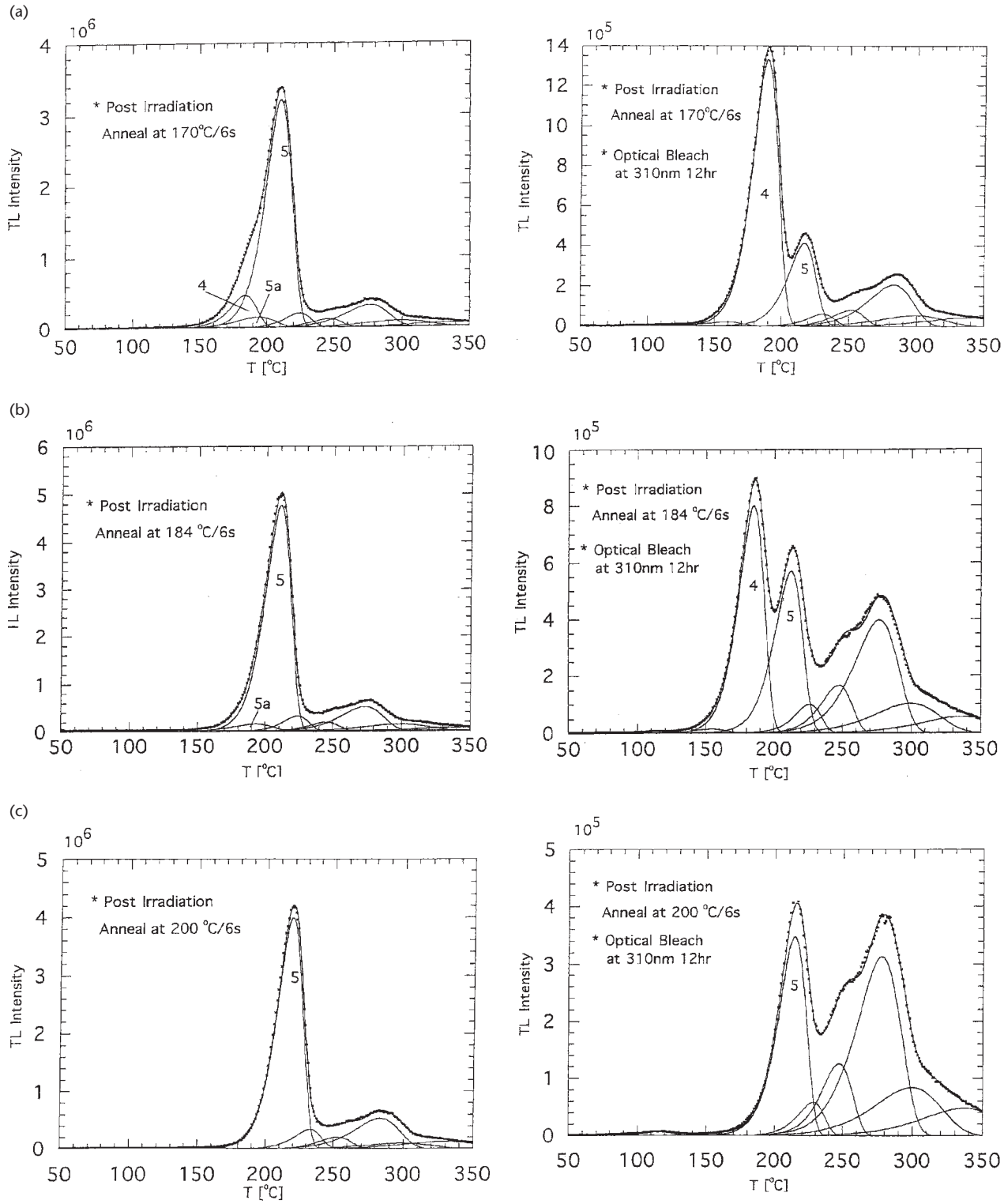

Figure 10. Glow curves illustrating the effect of optical bleaching at 4 eV (310 nm) and following three different pulsed (6 s) post-irradiation annealing temperatures: (*a*) 170˚C, (*b*) 184˚C, (*c*) 200˚C. At the lower temperatures, peak 4-traps are strongly repopulated following the bleach and peak 4 becomes the dominant peak in the glow curve. At 200˚C when peak 5a is totally erased by the post-irradiation anneal, peak 4 is almost not regrown/influenced by the bleach. The CE of peak 5 to peak 4 is measured at 0.0029 for this particular glow curve (previously published as figure 2 in Horowitz *et al* [27]).

cannot arise from a single/unique trapping structure with a temperature independent recombination mechanism, but must rather arise from a more complex mixture of TC/LC configurations and recombination mechanisms. We explain this dramatic difference in the CEs of peaks 5a and 5 as arising naturally from the difference in the charge trapping configuration following irradiation giving rise to these two peaks. As previously discussed, peak 5a is believed to arise

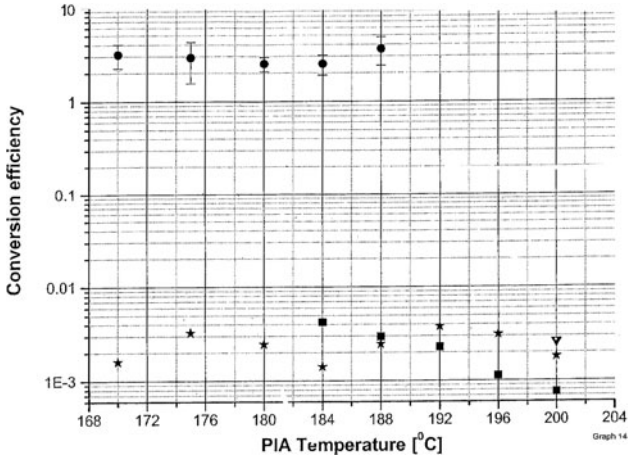

Figure 11. CEs as a function of the temperature of the post-irradiation anneal of peaks 5 to peaks 2 (⋆), 3 (■), 4 (▼) and of peak 5a to peak 4 (●). Note that the CE of peak 5a to peak 4 is three orders of magnitude greater than the CE of peak 5 to peak 4 due to the direct process involved in the optical conversion of peak 5a traps (trapped e–h) to peak 4 traps (trapped hole only) (previously published as figure 3 in Horowitz *et al* [27]).

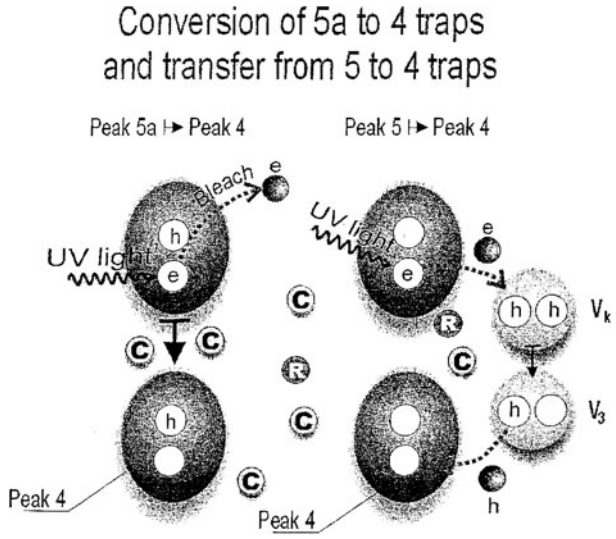

Figure 12. Effect of optical bleaching on the configuration states following irradiation. During bleaching, 310 nm light excites the electrons from the e–h occupied complex and the remaining hole transforms the TC/LC configuration into an occupied peak 4 trap. (previously published as figure 2 in Horowitz *et al* [12]).

from the TC/LC complex which has captured an e–h pair (figure 8); peak 5 arises from the same configuration which has captured an electron only and peak 4 arises from the same configuration which has captured a hole-only. The evidence supporting the identification of peak 4 as a hole-only configuration has been reviewed in the literature [30]. An example of such evidence can be seen in the experimental observation that following sensitization and illumination at 225 nm for 2 h (F band bleach), peak 5 is strongly repopulated due to capture of electrons from the CB. On the other hand there is no sign of an increase in the intensity of glow peak 4. The very high CE of peak 5a to peak 4 is now easily understood. Illumination by 310 nm light liberates an electron from the trapped e–h, a trapped hole remains, thus creating a peak 4 trap. This is a direct process (figure 12). No CB competitive processes are involved, therefore, the high CE. Liberation of an electron from the electron-only occupied complex (peak 5) leads to peak 4 only via CB transport mechanisms which are subject to competitive processes, therefore, the far lower CE. For example, the conversion from peak 5 to peak 4 might occur in the following manner. Electrons released from peak 5 traps are captured by V_3 centres (a pair of self-trapped holes) which release holes and are converted to V_k centres (a self-trapped hole; two nearest neighbour halide atoms capture a hole and are displaced towards each other). The holes from the thermally unstable V_k centres (single hole centres) migrate in the valence band and are eventually captured by the unoccupied TC/LC complex, leading to the formation of peak 4. Such a multi-stage process involving charge carrier diffusion in both the conduction and valence bands would be highly inefficient due to competitive CB processes. The value greater than unity, of the CE of peak 5a to peak 4, is also easily explained. The CE is measured from changes in the glow curve intensities—however, the direct optical conversion of peak 5a acts on the entire reservoir of e–h occupied strongly occupied TC/LC complexes. The occupation probability of the e–h complexes relative to the occupation probability of the electron-only occupied complexes following irradiation may be considerably greater than the relative intensity of glow peak 5a in the glow curve. This however implies that the *intrinsic* radiative recombination probability of the e–h in the e–h occupied complex is considerably less than unity.

It is possible to suggest other mechanisms to explain the three order-of-magnitude decrease in the CE as a function of PIA temperature, e.g. a temperature dependent mechanism which subtly alters the TC/LC configuration, making conversion following high-temperature PIA far less likely. However, it is our opinion that the simplicity and intuitive appeal of the direct conversion versus CB mediated conversion, coupled with additional ancilliary evidence provided in the following, should lead to the conclusion that conversion of peak 5a to peak 4 is by direct optical excitation of the electron in the e–h occupied complex, leaving behind a hole-only (peak 4).

5.2. HCP TL sensitivity following sensitization

The sensitivity of composite peak 5 to ^{60}Co gamma rays at low dose (in the linear part of the dose response) is increased by approximately a factor 10 by the following sensitization process: irradiation to a gamma dose level of 1000 Gy followed by a post-irradiation anneal of 280–300°C for 15–60 min. The increase in sensitivity (S/S_0) is attributed to the combined action of the partial filling/inactivation of the competitive centres (CCs) as well as an increase in the number of active/populated LCs [28]. It is important to note that peak 4 is not sensitized; indeed the opposite is true and peak 4 is 'desensitized', i.e. is not observed at all in completely sensitized material. This is additional evidence that peak 4 arises from hole-only capture in the TC/LC structure following irradiation since it is believed that the electron-filled (de-activated) CCs to peak 5 are transformed to active CCs for holes, thereby decreasing peak 4 sensitivity. Recently Horowitz *et al* [32] have measured $S/S_0 = 2 \pm 0.2$ (1 SD) for peak 5 following irradiation by 6.8 and 2.6 MeV He

ions. The sensitivity of peak 5a, however, does not increase at all, $S/S_0 = 0.86 \pm 0.12$ (1 SD). This again illustrates the very different nature of the TC/LC configuration giving rise to peak 5a, i.e. localized e–h occupation of the TC/LC structure since it is expected that the efficiency of the localized recombination mechanism would not be influenced by the changes in the population level of the competing centres brought about by the sensitization procedure. The increase in activated LCs does not increase the intensity of glow peak 5a due to the full occupation level of the strongly coupled TC/LC pairs in the HCP track core.

5.3. He ion TL fluence response: interpretation using the extended track interaction model

The TL fluence response of peaks 5a, 5 and 5b has been measured for 2.6 and 6.8 MeV He ions in both normal and sensitized LiF : Mg,Ti (TLD-100) [10, 32]. The behaviour of the TL fluence response of peak 5a compared to peaks 5 and 5b strongly supports the geminate recombination model for peak 5a. In sensitized material, the 2.6 and 6.8 MeV He ion TL fluence response clearly demonstrate a later entry into saturation for peak 5a (figure 13). For example, at $n = 3 \times 10^{11}\,\mathrm{cm}^{-2}$, the normalized TL fluence response $f(n) = 0.1$ and 0.95 for peaks 5 and 5a, respectively. Analysis using the extended track interaction model (ETIM) resulted in the following values for the track radial saturation parameter; $(r_{50})_{5a} = 10 \pm 2\,\mathrm{nm}$, compared to $(r_{50})_5 = 38 \pm 3\,\mathrm{nm}$ [32]. r_{50} is the distance from the HCP track axis at which there is a 50% TC/LC occupation probability and it is expected that $(r_{50})_{5a}$ (arising from high ionization density) would be substantially smaller than $(r_{50})_5$. In addition, the low value of 0.1 for the 'track-escape' parameter, N_e/N_w, of peak 5a deduced from ETIM analysis of He ion TL fluence response

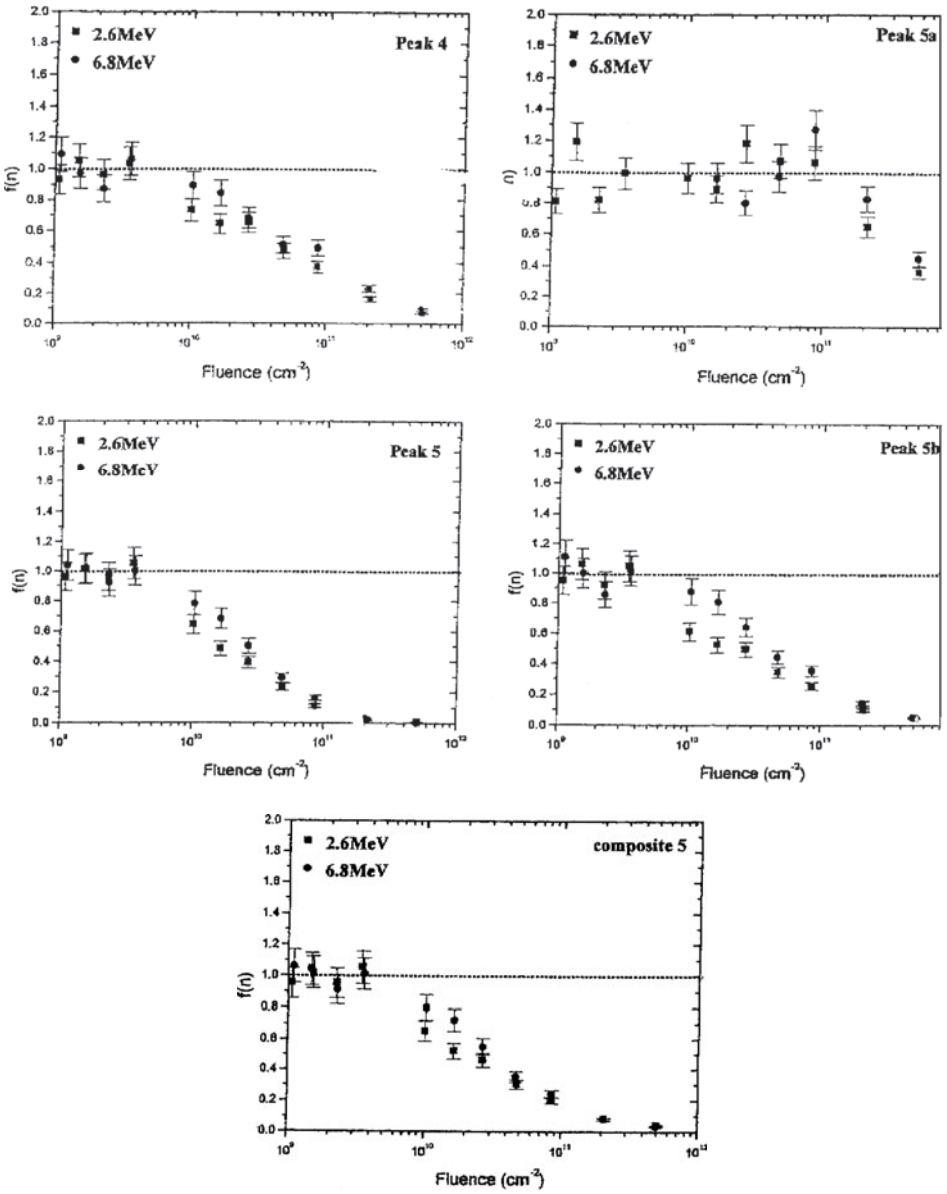

Figure 13. 2.6 and 6.8 MeV He ion TL fluence response in sensitized TLD-100 for glow peaks 4, 5a, 5, 5b and composite peak 5. Note the late entry into saturation of peak 5a.

compared to order of magnitude greater values for peaks 5 and 5b. N_e is the number of electrons which escape the HCP track and N_w is the number recombining within the track to produce TL photons. Since peak 5a is created preferentially in the track 'core' due to the 100% population of the TCs and LCs, it is expected that N_e/N_w would be small for peak 5a due to the decreasing probability of escape from the track as the distance from the track axis decreases. Finally, we should mention that additional evidence for spatially correlated TC/LC mechanisms in the TL of composite peak 5 in LiF : Mg,Ti (TLD-100) has been recently reviewed in some detail by Oster and Biderman [33].

5.4. Non-linear effects in the TL dose response

The dose response of many TL dosimetry materials can be characterized by a linear region of response at low dose, followed by a supralinear, and then sublinear region (figure 14). An interesting feature of the dose response in LiF : Mg,Ti (TLD-100) is the dependence of the extent of the supralinearity on ionization density when irradiated with low ionization density gamma rays or electrons as compared to HCPs of high ionization density. In addition, the maximum value of the supralinearity is strongly dependent on photon energy. This ionization density dependence of the supralinearity in other TL materials has not been extensively studied but is probably a common property of the dose response of many TL materials. The basic idea of the UNIM is that the linear response at low dose arises from geminate recombination in a localized entity. For gamma rays and electrons, the localized entity is the coupled/spatially correlated TC/LC pair [22, 30–32]. Note that the supralinearity is not present in LiF : Mg,Cu,P (a linear/saturating dose response is observed—figure 14) due to the absence of Ti and, consequently, the lack of formation of the TC/LC coupled pairs. The localized recombination process is unaffected by competitive processes and may occur via a 'tunnelling' mechanism between the TC and the LC in which the CB is not involved or via quasi-localized

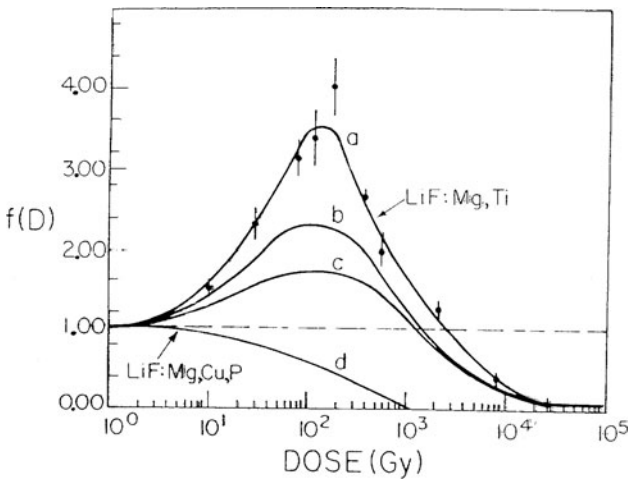

Figure 14. The normalized TL dose response $f(D)$ following photon irradiation at various energies: (a) ^{60}Co, (b) 50 kVp x-rays, (c) 20 kVp x-rays, (d) LiF : Mg, Cu, P following ^{60}Co irradiation (previously published as figure 1 in Horowitz Y S 1990 *Radiat. Prot. Dosim.* **33** 75-81).

recombination involving short-range charge carrier migration in the CB. Recombination between more distant higher order—nearest neighbour localized TC/LC entities involves long-range diffusion in the CB and is suppressed due to competitive processes (e.g. charge carrier capture by non-LCs). At higher dose levels, the average of the distance distribution between occupied/active neighbouring TC/LC entities decreases and the luminescence recombination efficiency thereby increases due to an increased probability of charge carrier migration between neighbouring localized entities resulting in an increased TL efficiency (supralinearity). In addition, if the CCs, during irradiation, capture charge of the same sign as the TCs, and are not depopulated during glow curve heating (so-called 'deep traps'), their 'competitive efficiency' is decreased as the dose level increases. This latter case is believed to be the case for composite peak 5 in LiF : Mg,Ti (TLD-100). The UNIM (and in its HCP form—the ETIM) is currently unique among existing models of TL dose response in its ability to quantitatively describe both low ionization density (gamma ray and electron) and high ionization density (HCP) TL dose response in a common/unifying mathematical framework. Previous applications of the UNIM have illustrated its capability to successfully quantitatively describe the following characteristics of gamma induced supralinearity for composite peak 5 in TLD-100.

- The dependence of the supralinearity on ionization density (gamma ray/electron energy) [11, 22, 30, 31] due to an energy dependent variation in the relative number of geminate recombination processes (not subject to competition) and CB mediated processes (subject to competition). This arises due to a dependence on ionization density on the relative number of electron/hole occupied TC/LC complexes following irradiation (configuration I in figure 8).
- The dependence of the supralinearity on heating rate (average recombination temperature) [34] due to differences in the dependence of the CC and LC cross-sections on temperature. Although both types of centres serve as recombination centres, only the LCs result in TL light emission.
- The lack of constraints (e.g. early or late entry into saturation) on the dose-dependence of the competitor required to explain the supralinearity of peak 5 [31]. It is demonstrated that the competitor need not enter into early saturation in order to promote supralinearity.

In the UNIM the TL signal intensity (the area under the glow peak) is given by

$$F(D) = ksn_e + (1 - ks)n_e \sum \int g(r_h, R_i) \exp\left(-\frac{R_i}{\lambda}\right) \times P_i(n_{LC}, R_i)\, dR_i, \quad (2)$$

k is the relative probability of geminate/localized recombination in the surround of the TC/LC complex not subject to competitive processes and s is the fraction of TC/LC complexes which have captured an e–h pair following irradiation. n_e is the number density (cm^{-3}) of occupied TCs and is given by $N_e[1 - \exp(-\beta_{TC}D)]$ as demonstrated by optical absorption studies, where β_{TC} is the dose filling constant of the TC and N_e is the total number of available TCs. r_0 is the radius of

the TC/LC pair and is some measure of the average distance over which geminate recombination can occur. $g(r_h \cdot R_i)$ is a three-dimensional solid angle factor between two neighbouring TC/LC pairs , $S_{LC} = \pi r_h^2$ is the cross-section for capture of an electron by the LC. R_i is the distance between neighbouring TC/LC pairs: λ, the mean free path of the electrons between the TC/LC pairs, is an increasing function of dose (due to the filling (de-activation) of the competitors with increasing dose) and is given by $\lambda = \lambda_0 \exp(\beta_{cc} D)$ where $\lambda_0 = (N_{cc} S_{cc})^{-1}$. β_{cc} is the dose filling constant of the CC, N_{cc} is the total number of available CCs and S_{cc} is the cross-section for charge carrier capture by the CC. $P_i(n_{LC}, R_i)\,\mathrm{d}R_i$ is the ith nearest-neighbour distance probability distribution function, and n_{LC} is the number density of occupied (active) LCs at dose D. The first term in equation (2) thus represents the linear/exponentially saturating part of the dose response which arises due to the lack of competitive processes. The second term describes the supralinear contribution which increases with dose above D_c, where the sum is over the first, second and third nearest-neighbour-interactions. The integral in equation (2) for composite peak 5a supralinearity is thus evaluated from r_0 (a few tens of angstroms) to a value of R_{max} of a few thousand angstroms.

In figure 8, the relation $k = k^* + b(1 - k^*)$ is demonstrated, where k^* is the fraction of processes leading to geminate recombination between a locally trapped e–h without involvement of the CB. The fraction $1 - k^*$ of the trapped electrons in configuration I escape to the CB upon heating and $b(1 - k^*)$ also recombine locally and are not subject to competitive processes. The fraction $(1 - k^*)(1 - b)$ are subject to competitive processes and may in fact be indistinguishable from electrons released from configuration II. At low dose levels (in the linear part of the dose response region), the processes represented by k^*, and $(1-k^*)b$ are postulated to give rise to peaks 5a and 5, respectively. A theoretical fit to the TL dose response of composite peak 5 is shown in figure 15 using $ks = 0.07$ indicating the relative number of strongly coupled TC/LC complexes undergoing geminate recombination and thereby resulting in TL light at low dose levels and a linear dose response.

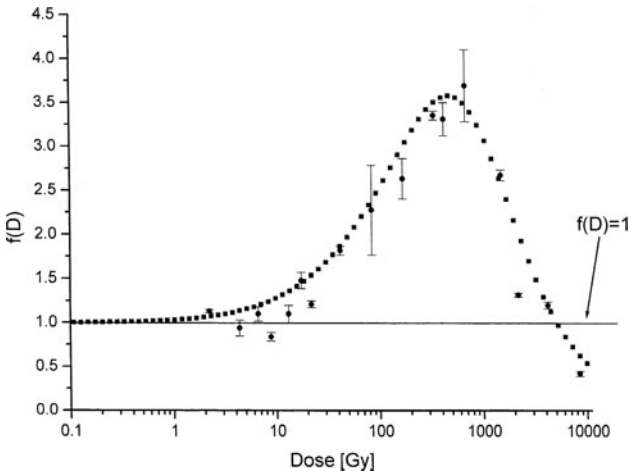

Figure 15. Theoretical fit to $f(D)$ following ^{60}Co irradiation using the UNIM. The parameters employed were: $\beta_{TC} = 1.1 \times 10^{-3}$ Gy^{-1}, $\beta_{LC} = 3.5 \times 10^{-3}$ Gy^{-1}, $\beta_{cc} = 1.0 \times 10^{-4}$ Gy^{-1}, $ks = 0.07$, $r_0 = 2 \times 10^{-9}$ m, $S_{LC} = 6 \times 10^{-16}$ m^2, $\lambda = 475 \times 10^{-10}$ m, $N_{LC} = 3 \times 10^{22}$ m^{-3}.

6. The ionization density dependence of glow peak 5a

Characterization of the dependence of the ratio 5a/5 on radiation type was carried out at the radiological research acceleration facility (RARAF) belonging to the Nevis Laboratory of Columbia University and the results are shown in table 1. The purpose of the experiment was to measure the peak ratio 5a/5 under various conditions of highly controlled and radiobiologically characterized HCP irradiations. This was considered as a first step in building up an experimental data base which may allow implementation of the peak 5a/5 device as a quasi-tissue-equivalent solid-state nanodosimeter. The results for each radiation field are based on the average of four measurements. Several points are worthy of mention: (i) there is a small but not insignificant energy dependence, i.e. the 5a/5 ratio increases with decrease in energy—this is expected due to the increasing relative importance of the track core (the relative track volume in which all the TCs and LCs are fully populated) as the HCP energy decreases. This point is illustrated in figure 16 showing track segment dose deposition profiles in condensed phase LiF. A radial dose level of 1000 Gy corresponds approximately to the full occupation level of the TCs and LCs. The relative importance of the track core clearly increases with decreasing ion energy. A theoretical model is being developed to predict 5a/5 ratios as a function of particle type using occupation probability radial distribution profiles based on Monte Carlo HCP radial dose distributions in condensed phase LiF [10] and optical absorption data [28]. (ii) The 5a/5 ratio is not correlated to average LET, re-inforcing the inadequacy of the LET concept in prediction the effects of ionization density in TL solid-state systems. (iii) The 5a/5 ratio is largely insensitive to particle type or energy (all the measured values fall within 1 SD of the average). This could be a significant advantage in certain applications because it could lead to a separation of the 'high' versus 'low' ionization density component of the radiation field irrespective of the particulars of the mixed radiation field. Having presented the considerable evidence supporting the premise that peak 5a arises from a localized e–h pair in a strongly coupled TC/LC system, it is now possible to explain the increased presence of peak 5a in HCP and neutron irradiated samples. Geminate recombination is of much higher probability in the HCP ion

Table 1. Peak 5a/5 ratios in high ionization density radiation fields.

Radiation	Energy (MeV)	LET in H_2O (keV micron^{-1})	5a/5	1 SD
Alpha[a]	5.16	95	0.21	0.04
Alpha	2.17	188	0.30	0.05
Protons	3.65	10	0.22	0.01
Protons	0.54	42	0.26	0.04
Deuterons	3.5	64	0.20	0.03
Deuterons	0.8	20	0.27	0.04
Neutrons[b]	14	—	0.21	0.06
Neutrons	0.21	—	0.21	0.09
Overall average	0.23 ± 0.05			

[a] Particle irradiations were carried out a fluence of 10^{10} p cm^{-2} in a parallel beam configuration.
[b] Neutron dose level of 1 Gy.

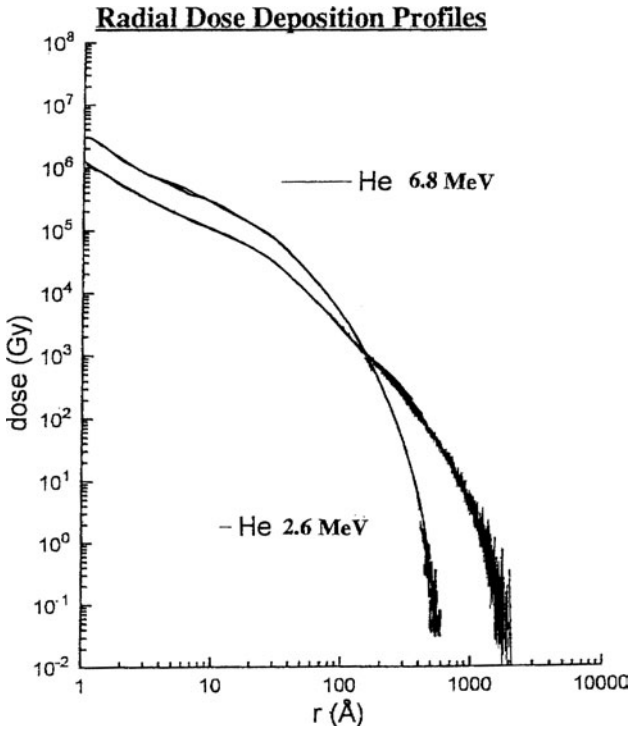

Figure 16. Radial dose profiles calculated via Monte Carlo in condensed phase LiF for 2.6 and 6.8 MeV He ions. The main difference between the two energies is the much greater dose deposition for 6.8 MeV He ions at radial distances greater than approximately 15 nm.

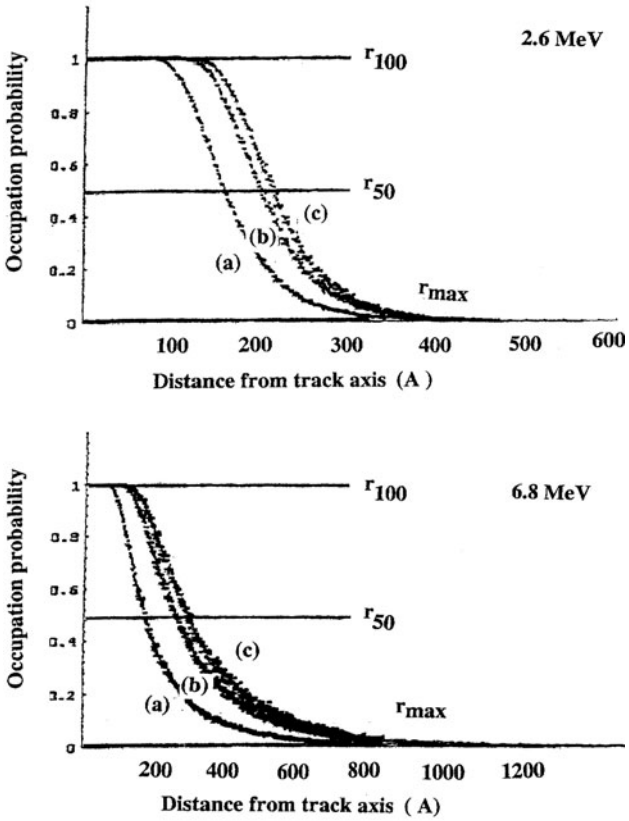

Figure 17. (*a*) Radial defect occupation probabilities for 2.6 and 6.8 MeV He ions in LiF for various values of ß (the dose filling constant measured from optical absorption studies) from (*a*) 0.9×10^{-3} Gy^{-1} (*b*) 3.5×10^{-3} Gy^{-1}, (*c*) 6×10^{-3} Gy^{-1}. These range of value encompass the expected values for the TCs and LCs giving rise to composite peak 5 (previously published as figure 3 in Horowitz *et al* [12]).

track due to the extremely high dose levels in the track core (figure 17) leading to a higher probability of simultaneous e–h population of the nearest-neighbour TC/LC correlated entity. As can be seen in figure 18, the TCs and LCs are fully populated out to a radial distance of approximately 15–20 nm from the He ion track axis—thus ensuring increased efficiency in the creation of peak 5a. In the 5 MeV He ion induced glow curves (following a post-irradiation anneal to remove peaks 2 and 3) the relative intensity of peak 5a to peak 5 is $[5a/5]_H = 0.21 \pm 0.03$ (1 SD) (figure 19). However, as previously mentioned, its relative intensity in gamma induced glow curves (low ionization density irradiation) is $[5a/5]_L = 0.008 \pm 0.008$ (1 SD). The high temperature glow peaks in LiF : Mg,Ti (peaks 6–9) show what appears to be a similar behaviour. That is, an enhanced presence following HCP and neutron irradiation. However, we believe that this latter behaviour is for an entirely different reason. The high temperature glow peaks arise from delocalized recombination mechanisms. Their increased presence following HCP irradiation arise from the combined effects of high radial dose and the reduced cross-section of the competing centres (relative to the LCs) at the high temperatures corresponding to peaks 6–9. To support this statement one need only point out that the relative intensity of peaks 6–9 in gamma irradiated glow curves at high dose is similar to that of HCP generated glow curves. It should be also pointed out that the high temperature peaks do not increase following the 310 nm bleach (figure 10—the reader should note the change in the vertical scale of the glow curve following the 310 nm bleach). Contrary to the behaviour of peak 5a, there is thus no evidence to suggest that peaks 6–9 arise from localized TL mechanisms. The peak 5a/5 relative intensity ratio (high ionization density to low ionization density) $[5a/5]_{H/L} = 2$–3 for low energy HCPs is thus a measure of the effect of ionization density on the relative number of 'double-energy-transfer-events' to 'single-energy transfer-events' in a nanometric sized volume and is therefore the conceptual analogue to the effects of ionization density on the yield of DSBs in DNA.

7. Conclusion

We have demonstrated the significant effects of ionization density on the TL properties of composite peak 5 in LiF : Mg,Ti. These effects arise due to localized e–h capture in nanoscale sized TC/LC correlated pairs. In addition we promote the concept of using existing molecular nanostructures in TL solid-state materials as solid-state quasi-tissue-equivalent nanodosimeters. The concept is based on mimicking radiobiology (specifically the ionization density dependence of DSBs in DNA) by using the similar ionization density dependence of simultaneous e–h capture in spatially correlated TC/LC pairs (of approximately the same dimensions as the DNA molecule) in the TL of LiF : Mg,Ti. This simultaneous e–h capture has been shown to lead to

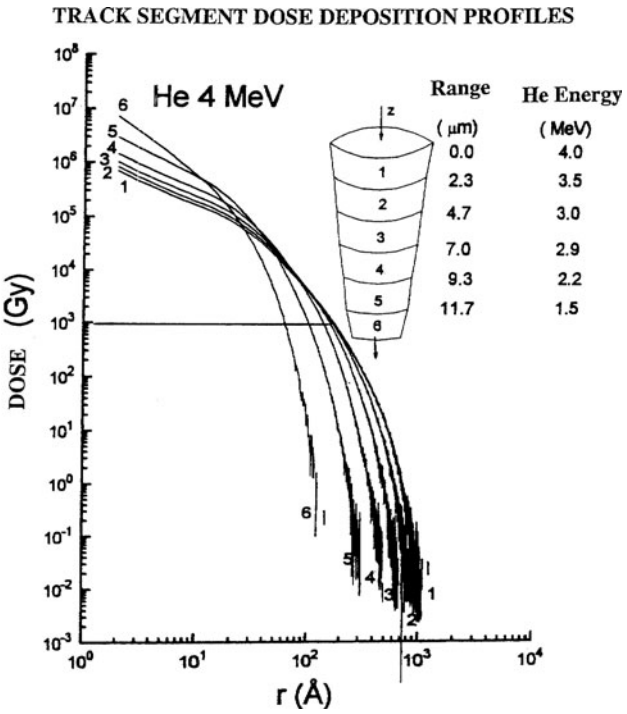

Figure 18. Track segment dose deposition profiles calculated by Monte Carlo for 4 MeV He ions stopping in condensed phase LiF. The dose is shown as a function of radial distance from the track axis. The horizontal line at 1000 Gy indicates the dose level corresponding to approximately full occupation of the TCs and LCs in the He ion track.

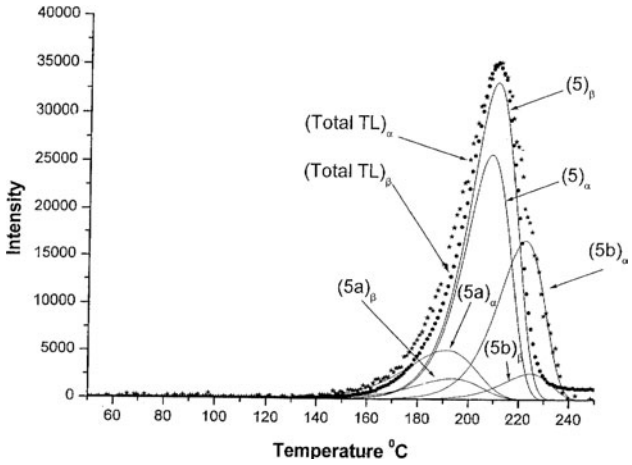

Figure 19. Typical gamma and He ion induced glow curve of TLD-100 following post-irradiation annealing of 182°C for 6 s to remove the low-temperature peaks. The fit shows peaks 5a, 5 and 5b using a first-order kinetics model for the peak shapes. The high temperature structure centred at approximately 270°C, observed following HCP and high dose gamma irradiation, has been subtracted.

localized/geminate recombination and to an ionization density dependence in the relative intensity of peak 5a to peak 5 of $[5a/5]_{H/L} = 2$–3 similar to the dependence of DSBs on ionization density as reported by Kampf [4]. Hence the peak 5a/5 nanodosimeter. What remains to be carried out is the establishment of an empirical correlation between the ratio of peak 5a to peak 5 in a variety of mixed neutron/gamma radiation fields and/or HCP radiation fields of known RBE. We are also developing a model based on modified track structure theory (MTST—[10]) which will allow the estimation of the ratio of peak 5a/5 for various ion types and energy to be compared with the experimental data shown in table 1. As previously noted peak 5a is created preferentially in the track core (100% occupation of the TCs and LCs) and with decreasing probability with increasing radial distances from the track axis. Calculation of the creation probability of peak 5 luminescence which is expected to occur mainly outside the track core, requires knowledge of the ratio of the CC capture cross-section to the LC capture cross-section. The success of the model will be largely determined by the ability of a single value of the cross-section ratio parameter to correctly predict the 5a/5 ratio for a large variety of particle types and energies. Further improvements are also required in the precision of measurement of the ratio 5a/5 in order to extend the application to mixed radiation fields with a dominant low ionization density component. This might then allow nanodosimetric measurements of dose and estimation of certain radiobiological end-points without any further need for characterization of the radiation interaction parameters of the radiation field.

Acknowledgments

This research was partially supported by a grant from the United-States–Israel BiNational Science Foundation (BSF), Jerusalem, Israel: Contract 9800014.

References

[1] Maurer R H, Charles H K Jr and Pisacane V L 2002 Advances in space technology: the NSBRI technology development team *Radiat. Prot. Dosim.* **100** 479–87
[2] Fry R J M 2002 Radiations in space: risk estimates *Radiat. Prot. Dosim.* **100** 475–7
[3] Powell S and McMillan T J 1990 DNA damage and repair following treatment with ionizing radiation *Radiotherapy Oncol.* **19** 95–108
[4] Kampf G 1988 Induction of DNA double strand breaks by ionising radiation of different quality and their relevance for cell inactivation *Radiobiol. Radiotherapy* **29** 631–58
[5] Pouget J P, Frelon S, Ravanat J L, Testard I, Odin F and Cadet J 2002 Formation of modified DNA bases in cells exposed either to gamma radiation or to high-LET protons *Radiat. Res.* **57** 589–95
[6] Rossi H H and Zaider M 1996 *Microdosimetry and its Applications* (Berlin: Springer)
[7] Nikjoo H and Charlton D E 1995 Calculations of range and distribution of damage to DNA by high and low LET radiations *Radiation Damage in DNA* ed A F Fuciarelli and J D Zimbrick (Columbus, OH: Battelle Press) pp 29–41
[8] Zaider M, Dicello J F and Horowitz Y S 1999 Where do we stand on solid state microdosimetry *Radiat. Prot. Dosim.* **82** 163–6
[9] Baum S J 1978 *Organic and Biological Chemistry* (London: Macmillan)
[10] Horowitz Y S, Avila O and Rodriguez-Villafuerte M 2001 Theory of heavy charged particle response (efficiency and supralinearity in TL materials) *Nucl. Instrum.* B **184** 85–112
[11] Kraft G, Taucher-Scholz G and Heilmann J 1995 LET-effects in DNA *Radiation Damage in DNA* ed A F Fuciarelli and J D Zimbrick (Columbus, OH: Battelle Press) pp 203–14
[12] Horowitz Y S, Oster L, Satinger D, Biderman S and Einav Y 2002 The composite structure of peak 5 in the glow curve of LiF : Mg,Ti (TLD-100): confirmation of peak 5a arising

from a locally trapped electron–hole configuration *Radiat. Prot. Dosim.* **100** 123–6
[13] Stoebe T G and Watanabe S 1975 Thermoluminescence and lattice defects in LiF : Mg,Ti *Phys. Status Solidi* a **29** 11
[14] McKeever S W S and Horowitz Y S 1990 Charge trapping mechanisms and microdosimetric processes in LiF *Radiat. Phys. Chem.* **36** 35–46
[15] Stoebe T G and Morgan M D 1984 Models of TL trapping and recombination centers *Thermoluminescence and Thermoluminescent Dosimetry* vol I, ed Y S Horowitz (Boca Raton: CRC press)
[16] Townsend P D, Ahmed K, Chandler P J, McKeever S W S and Whitlow H J 1983 Measurements of the emission spectra of LiF during thermoluminescence *Radiat. Effs.* **72** 245–57
[17] Biderman S, Horowitz Y and Oster L 2002 Investigation of the emission spectra of LiF : Mg,Ti (TLD-100) during thermoluminescence *Radiat. Prot. Dosim.* **100** 369–72
[18] Weizman Y, Horowitz Y S, Oster L, Yossian D, Bar-Lavy O and Horowitz A 1998 Mixed-order kinetic analysis of the glow curve characteristics of single crystal LiF : Mg,Ti as a function of Ti concentration *Radiat. Meas.* **29** 517–25
[19] Horowitz Y S, Satinger D, Yossian D, Brandan M E, Buenfil A E, Gamboa-deBuen I, Rodriguez-Villafuerte M and Ruiz C G 1999 Ionization density effects in the thermoluminescence of TLD-100: computerised T_m–T_{stop} glow curve analysis *Radiat. Prot. Dosim.* **84** 239–42
[20] Biderman S, Horowitz Y S, Oster L, Einav Y and Dubi Y 2002 Glow curve analysis of composite peak 5 in LiF : Mg,Ti (TLD-100) using optical bleaching, thermal annealing and computerized glow curve deconvolution *Radiat. Prot. Dosim.* **101** 69–72
[21] Delgado A and Gomez-Ros J 1988 An interpretation of the isothermal decay associated with peaks IV and V in the TL of LiF-TLD *J. Phys. D: Appl. Phys.* **21** 652–6
[22] Mahajna S and Horowitz Y S 1997 The unified interaction model applied to the gamma ray induced supralinearity and sensitisation of peak 5 in LiF : Mg,Ti (TLD-100) *J. Phys. D: Appl. Phys.* **30** 2603–19
[23] Townsend P D and Rowlands A P 1999 Extended defect models for thermoluminescence *Radiat. Prot. Dosim.* **84** 7–12
[24] Horowitz Y S 1999 The average distance between Mg-based trapping structures in LiF : Mg,Ti and LiF : Mg,Cu, P and the relevance to microdosimetry *Radiat. Prot. Dosim.* **82** 51–4
[25] Visocekas R 2002 Tunneling in afterglow, its coexistance and interweaving with thermally stimulated luminescence *Radiat. Prot. Dosim.* **100** 45–9
[26] Weizman Y, Horowitz Y S and Oster L 1999 Investigation of the composite structure of peak 5 in the thermoluminescent of glow curve of LiF : Mg,Ti (TLD-100) using optical bleaching *J. Phys. D: Appl. Phys.* **32** 2118–27
[27] Horowitz Y S, Einav Y, Biderman S and Oster L 2002 Localised and delocalised optically induced conversion of composite glow peak 5 in LiF : Mg,Ti (TLD-100) to peak 4 as a function of post-irradaition annealing temperature *Radiat. Prot. Dosim.* **100** 135–8
[28] Issa N, Horowitz Y S and Oster L 2001 Optical absorption in LiF : Mg,Ti and its relationship to thermoluminescence and thermoluminescence dose response *Radiat. Meas.* **33** 491–6
[29] McKeever S W S 1984 Optical absorption and luminescence in LiF : TLD-100 *J. Appl. Phys.* **56** 2883–9
[30] Horowitz Y S, Mahajna S, Oster L, Weizman Y, Satinger D and Yossian D 1998 The unified interaction model applied to the gamma induced supralinearity and sensitisation of peaks 4 and 5 in LiF : Mg,Ti (TLD-100) *Radiat. Prot. Dosim.* **78** 169–93
[31] Nail I, Horowitz Y S, Oster L and Biderman S 2002 The unified interaction model applied to composite peak 5 in LiF : Mg,Ti (TLD-100): properties of the luminescent and competitive centers during sensitisation *Radiat. Prot. Dosim.* **102** 295–304
[32] Horowitz Y S, Satinger D, Oster L, Brandan M E, Avila O, Rodriguez-Villafuerte M, Gamboa-deBuen I, Buenfil A E and Ruiz-Trejo C 2001 The extended track interaction model: supralinearity and saturation He ion TL fluence response in sensitised TLD-100 *Radiat. Meas.* **33** 459–73
[33] Oster L and Biderman S 2002 New evidence for spatially correlated TC–LC mechanisms in the thermoluminescence of LiF : Mg,Ti *Radiat. Prot. Dosim.* **100** 191–8
[34] Horowitz Y S, Satinger D and Oster L 1999 The dependence of dose response supralinearity of peak 5 in TLD-100 on recombination temperature *Radiat. Prot. Dosim.* **84** 99–102